cells possess two anterior margins. The dorsal-ventral polarity of wild-type egg chambers is specified by the localization of gurken mRNA to the dorsal-anterior corner of the oocyte, adjacent to the nucleus (Fig. 3G) (*21*). In bipolar oocytes, gurken mRNA still accumulates above the nucleus, regardless of which end of the cell it lies (Fig. 3H). The localization of *gurken* transcripts therefore seems to be directed by the position of the oocyte nucleus and is not dependent on the duplicated microtubule cytoskeleton that localizes bicoid and oskar mRNAs.

On the basis of our observations, we propose that AP polarity in *Drosophila* originates with the movement of the oocyte to the posterior of the germline cyst, a process that requires the products of the *spindle-C*, *dicephalic*, and *armadillo* (*22*) genes, and at least three other loci on the third chromosome (*23*). This initial arrangement of the germline cells then determines all subsequent events in the establishment of anterior-posterior asymmetry in the egg chamber. To reconcile this model with the role of the follicle cells in the localization of maternal mRNAs in the oocyte, we suggest that the oocyte first induces posterior fate in the adjacent polar follicle cells, and that these follicle cells then signal back to the oocyte to reorganize the microtubule cytoskeleton, thereby defining AP polarity (Fig. 4). When this signaling fails, either as a result of the misplacement of the oocyte or a lack of somatic components required for the acquisition of follicle cell fate (*8*), the oocyte develops two anterior ends. Thus, like dorsoventral axis formation (*24*), the generation of anterior-posterior polarity involves signaling from the germ line to the somatic follicle cells, and from the follicle cells back to the germ line.

REFERENCES AND NOTES

1. D. St Johnston and C. Nüsslein-Volhard, *Cell* **68**, 201 (1992); A. Ephrussi and R. Lehmann, *Nature* **358**, 387 (1992).
2. T. Berleth *et al.*, *EMBO J.* **7**, 1749 (1988).
3. D. St Johnston, W. Driever, T. Berleth, S. Richstein, C. Nüsslein-Volhard, *Dev. Suppl.* **107**, 13 (1989).
4. J. Kim-Ha *et al.*, *Cell* **66**, 23 (1991); A. Ephrussi *et al.*, *ibid.*, p. 37.
5. W. E. Theurkauf, S. Smiley, M. L. Wong, B. M. Alberts, *Development* **115**, 923 (1992).
6. I. Clark *et al.*, *Curr. Biol.* **4**, 289 (1994).
7. N. J. Pokrywka and E. C. Stephenson, *Development* **113**, 55 (1991).
8. H. Ruohola *et al.*, *Cell* **66**, 433 (1991).
9. H. Ruohola-Baker, L. Jan, Y. Jan, *Trends Genet.* **10**, 89 (1994).
10. R. Tearle and C. Nüsslein-Volhard, *Drosophila Inf. Serv.* **66**, 209 (1987).
11. Other *spn-C* alleles, *spn-C*^{422} and *spn-C*^{660}, produce bipolar egg chambers with an identical phenotype to that produced by *spn-C*^{094}, although with a lower frequency (24 and 29%, respectively) (*25*). All the *spn-C* egg chambers shown are *spn-C*^{094}, except Fig. 3B which is *spn-C*^{422}.
12. M. Lohs-Schardin, *Wilhelm Roux's Arch. Dev. Biol.* **191**, 28 (1982).
13. A. Spradling, in *The Development of* Drosophila melanogaster, M. Bate and A. Martinez-Arias, Eds. (Cold Spring Harbor Laboratory Press, Cold Spring Harbor, New York, 1993), vol. 1, pp. 1–70.
14. A. Mahowald and M. Kambysellis, in *The Genetics and Biology of* Drosophila, M. Ashburner and T. Wright, Eds. (Academic Press, London, 1980), vol. 2d, p. 141.
15. D. Montell, P. Rorth, A. Spradling, *Cell* **71**, 51 (1992).
16. Germline clones were generated by irradiating with x-rays larvae of the genotype *ru spn-C*^{094} *st e ca/ P[ovo*^{D1}*]*^{2x48}, essentially as described [T.-B. Chou, E. Noll, N. Perrimon, *Development* **119**, 1359 (1993)]. We dissected 2500 females to find 11 visible clones in the ovaries. About 30% of the chimeric egg chambers showed the *spn-C* phenotype.
17. S. Goode, D. Wright, A. P. Mahowald, *Development* **116**, 177 (1992).
18. D. St Johnston, D. Beuchle, C. Nüsslein-Volhard, *Cell* **66**, 51 (1991).
19. E. Giniger, W. Wells, L. Jan, Y. Jan, *Roux's Arch. Dev. Biol.* **202**, 112 (1993).
20. H.-K. Cheung, T. Serano, R. Cohen, *Development* **114**, 653 (1992).
21. F. Neuman-Silberberg and T. Schüpbach, *Cell* **75**, 165 (1993).
22. M. Peifer, S. Orsulic, D. Sweeton, E. Wieschaus, *Development* **118**, 1191 (1993).
23. Mutations in the *spn-A, spn-B,* and *spn-D* genes (*10*) result in a very similar phenotype to *spn-C*, and in all cases the misplacement of the oocyte has the same consequences on the establishment of AP polarity in the egg chamber, as determined by the *slbo* expression in the follicle cells and the localization of osk and bcd mRNAs within the oocyte (*25*).
24. R. Chasan and K. Anderson, in (*13*), pp. 387–424.
25. A. González-Reyes and D. St Johnston, unpublished data.
26. Actin filaments were stained with rhodamine-labeled phalloidin as described [F. Xue and L. Cooley, *Cell* **72**, 681 (1993)]. The images from different focal planes were collected with the use of confocal microscopy.
27. For Hoechst staining, fixed ovaries were incubated 3 min with Hoechst (10 mg/ml, Sigma) and mounted in 70% glycerol. X-gal staining was as described (*15*).
28. The in situ hybridizations were performed as described [P. Ingham, *Nature* **366**, 560 (1993)] and immunohistochemistry as described (*18*). We used the transgenic line KZ32 as a source of kinesin–β-galactosidase protein (*6*).

29. We wish to thank I. Clark, R. Cohen, T.-B. Chou, D. Montell, F. Neuman-Silberberg, N. Perrimon, T. Serano, and T. Schüpbach for supplying us with fly strains and plasmids and for sharing unpublished results; O. Dunin-Borkowski for advice on protocols; N. Brown, J. Casanova, and M. D. Martín-Bermudo for comments on the manuscript; and M. Weston for Fig. 3E. We are also grateful to our colleagues in the lab for their helpful discussions and advice. A.G.-R. is a European Molecular Biology Organization postdoctoral fellow. This work was supported by a Wellcome Trust Senior Fellowship to D.StJ.

21 June 1994; accepted 25 August 1994

An AIDS-Like Condition Induced in Baboons by HIV-2

Susan W. Barnett, Krishna K. Murthy, Brian G. Herndier, Jay A. Levy*

Six baboons (*Papio cynocephalus*) were intravenously inoculated with the human immunodeficiency virus–type 2 (HIV-2) strain HIV-2_{UC2}. All seroconverted within 6 weeks after inoculation; five animals became persistently infected. Four developed lymphadenopathy, and three of the animals had $CD4^+$ T cell loss within 18 to 24 months after inoculation. One of these baboons, showing severe clinical symptoms, showed at necropsy widespread dissemination of virus with follicular depletion in the lymph nodes, extensive fibromatosis involving lymphoid and nonlymphoid tissues, and lymphocytic interstitial pneumonitis. Another animal is cachectic and exhibited lymphoid follicular lysis and fibrous skin lesions. Other baboons inoculated with a second strain, HIV-2_{UC14}, have shown evidence of persistent infection. HIV-2 infection of baboons provides a valuable animal model for studying HIV persistence and pathogenesis and for evaluating approaches to antiviral therapies.

Despite advances in our understanding of acquired immunodeficiency syndrome (AIDS) and its etiologic agents HIV-1 and HIV-2, there is no well-established animal model to study potential therapies and vaccines for HIV-induced diseases. Of the nonhuman primates, the chimpanzee (*1*) and the pig-tailed macaque *Macaca nemestrina* (*2*) are the major species susceptible to HIV-1 infection. Apart from some symptoms of acute infection observed in the macaque model, in neither of these systems have animals developed signs of disease. In the case of the chimpanzee, this fact, together with their endangered species status and cost (*3*), makes their clinical use problematic. Moreover, most evidence indicates that reproducible persistent infection of *M. nemestrina* with HIV-1 strains cannot be achieved (*4*).

Although HIV-2 infection was previously reported mostly in West African countries, there is now evidence of its presence in other parts of the world, par-

S. W. Barnett and J. A. Levy, Department of Medicine and Cancer Research Institute, School of Medicine, University of California, San Francisco, CA 94143, USA.
K. K. Murthy, Southwest Foundation for Biomedical Research, San Antonio, TX 78228, USA.
B. G. Herndier, Department of Pathology, School of Medicine, University of California, San Francisco General Hospital, San Francisco, CA 94110, USA.

*To whom correspondence should be addressed.

ticularly India (5). The HIV-2 subtype of human immunodeficiency viruses is molecularly and serologically distinct from HIV-1 strains. The two subtypes share only about 40% amino acid identity in their Env surface glycoproteins. In fact, HIV-2 strains appear to be more closely related to simian immunodeficiency virus (SIV) strains recovered from sooty mangabys in West Africa (SIV_{sm}) and captive macaques (SIV_{mac}) (6).

The most promising animal models presently being evaluated for studies of HIV pathogenesis and antiviral approaches are rhesus macaques infected with SIV_{mac} strains (7) and SIV_{mac}/HIV-1 chimeras (8). Nevertheless, despite the close relatedness of certain SIV and HIV-2 strains, results obtained with these SIV-based models may not be directly applicable to infection with a human lentivirus. In other models, HIV-2 infection of various macaque species has also been studied (9), but the virus showed pathogenicity only after serial passage through *M. nemestrina* (*10*). Therefore, an important need exists for a reproducible and affordable animal model of viral persistence and pathogenesis that can use various HIV strains to test possible vaccine and antiviral strategies. We show here that persistent infection of baboons can be readily achieved with diverse strains of HIV-2. In addition, some of the infected animals have exhibited symptoms and diseases analogous to those observed in HIV-infected humans.

Early pilot studies in our laboratory suggested that in vitro infection of nonhuman primate peripheral blood mononuclear cells (PBMCs) with HIV strains was predictive of successful infection in vivo (*11*). Two HIV-2 strains from Côte d'Ivoire ($HIV\text{-}2_{UC2}$ and $HIV\text{-}2_{UC3}$, referred to here as UC2 and UC3) (*12*) readily infected cultured baboon PBMCs and produced persistent infection in these same animals. Of the two viral strains, UC2 appeared to induce the longest period of persistent infection (for example, baboon 8198) (Table 1). For almost 4 years, beginning at 18 months after inoculation, this baboon has had persistent viremia and has exhibited a continuous decline in total $CD4^+$ T lymphocytes (Fig. 1A).

On the basis of these findings, we chose to inoculate additional baboons with the UC2 strain and to seek other HIV-2 isolates for animal inoculation. After we performed in vitro prescreening in baboon PBMCs, we identified two other HIV-2 strains, UC12 and UC14 (*13*), that also grew efficiently and consistently in cultured baboon PBMCs. The UC2 strain grew well in the PBMCs of 13 out of 13 (100%) of the baboons tested; UC12 grew in 11 out of 13 (84.6%) and UC14 in 13 out of 13 (100%).

Four additional baboons (9168, 9206, 9429, and 8387) were given an intravenous inoculation of approximately 5000 median tissue culture infectious doses ($TCID_{50}$) (measured in human PBMCs) of UC2. Within 2 weeks of virus inoculation, all four of these animals developed widespread lymphadenopathy (Table 1), which persisted for at least 20 weeks. At 1 year after inoculation, lymph node sections taken from one animal, 9206, revealed a mixed cellular hyperplasia that included follicular hyperplasia, paracortical hyperplasia, and infiltration of the medullary cords with plasma cells. Follicular hyperplasia is also commonly observed during the early stages of HIV and SIV infections (*14*).

Infectious virus was recovered from the PBMCs of all four UC2-inoculated baboons as early as 2 weeks after inoculation. Positive virus cultures were repeatedly demonstrated in three of the animals (9206, 9429, and 9168) (Table 1; Fig. 1, B and C). The PBMCs from the fourth animal, 8387, were shown to harbor provirus as late as 44 weeks after inoculation as determined by DNA polymerase chain reaction analysis (*15*). Seroconversion was observed in the baboons at 4 to 6 weeks after virus inoculation (Table 1; Fig. 1, B and C). Protein immunoblot analysis of sera from three of the UC2-infected baboons showed reactivity to all the major HIV-2 viral proteins within 12 to 20 weeks; the other baboon (8387) demonstrated only limited reactivity to p27 Gag protein.

Starting at about 65 weeks after inoculation, a dramatic loss of $CD4^+$ T lymphocytes was observed in baboon 9429 (Fig. 1B). During the next 6 months, this animal's total $CD4^+$ T cells dropped from an average of 2000 cells/mm^3 to only 600

Table 1. HIV-2 inoculation of *Papio cynocephalus* baboons. The animals used in these studies were young adult baboons (4 to 9 years old). Subspecies designations are PCA, *Papio cynocephalus anubis*; PCH, *Papio cynocephalus hamadrayas*; and PCX, *Papio cynocephalus anubis/cynocephalus*. Persistent infection indicates positive virus cultures from the PBMCs at almost all time points (>90%); intermittent virus isolation indicates positive virus cultures at more than one time point after acute infection (0 to 20 weeks) and at least one positive isolation within the last 4 months; transient isolation indicates virus recovery only during acute infection. Methods are as described (*25*).

Inoculation date	Baboon (subspecies)	Inoculum	Infection status (duration)	Clinical status (time of initial signs)
9/16/88	8198 (PCA)	UC2	Persistent infection (6 years) Seropositive (6 years)	$CD4^+$ cell decline (18 months)
1/23/92	9429 (PCH)	UC2	Persistent infection (2 years, 2 months) Seropositive (2 years, 2 months)	$CD4^+$ cell decline (16 months) Lymphadenopathy (2 weeks) AIDS-like syndrome (28 months)
	9206 (PCH)	UC2	Persistent infection (>2.5 years) Seropositive (>2.5 years)	$CD4^+$ cell decline (28 months) Lymphadenopathy (2 weeks) AIDS-like syndrome (32 months)
	9168 (PCH)	UC2	Intermittent virus isolation (>2.5 years) Seropositive (>2.5 years)	Lymphadenopathy (2 weeks)
	8387 (PCX)	UC2	Transient virus isolation (2 weeks) Seropositive (>2.5 years)	Lymphadenopathy (2 weeks)
	7796 (PCH)	Control	Uninfected Seronegative	
1/25/93	8513 (PCX)	UC14	Transient virus isolation (2 weeks) Plasma viremia (2 weeks) Seropositive (>1.5 years)	Transient $CD4^+$ cell decline (4 to 8 months)
	8570 (PCH)	UC14	Intermittent virus isolation (>1.5 years) Plasma viremia (2, 6, and 8 weeks) Seropositive (>1.5 years)	
	8594 (PCH)	UC14	Intermittent virus isolation (>1.5 years) Seropositive (>1.5 years)	

cells/mm^3, and its CD4$^+$/CD8$^+$ cell ratio decreased from an average of 1.5 to 0.3. During the same time period, the uninfected control baboon 7796 exhibited an average of about 1600 CD4$^+$ cells/mm^3 with a CD4$^+$/CD8$^+$ cell ratio of about 1.6. Moreover, approximately 2 years after inoculation with UC2, baboon 9429 had cachexia, marked lymphadenopathy, hepatosplenomegaly, lymphocytopenia, thrombocytopenia, severe anemia, skin lesions, and ulcerative gingivitis that did not respond to antibiotic treatment. This animal was subsequently killed, and its tissues were examined at necropsy. Total peripheral CD4$^+$ lymphocytes at the time of necropsy were at 275 cells/mm^3.

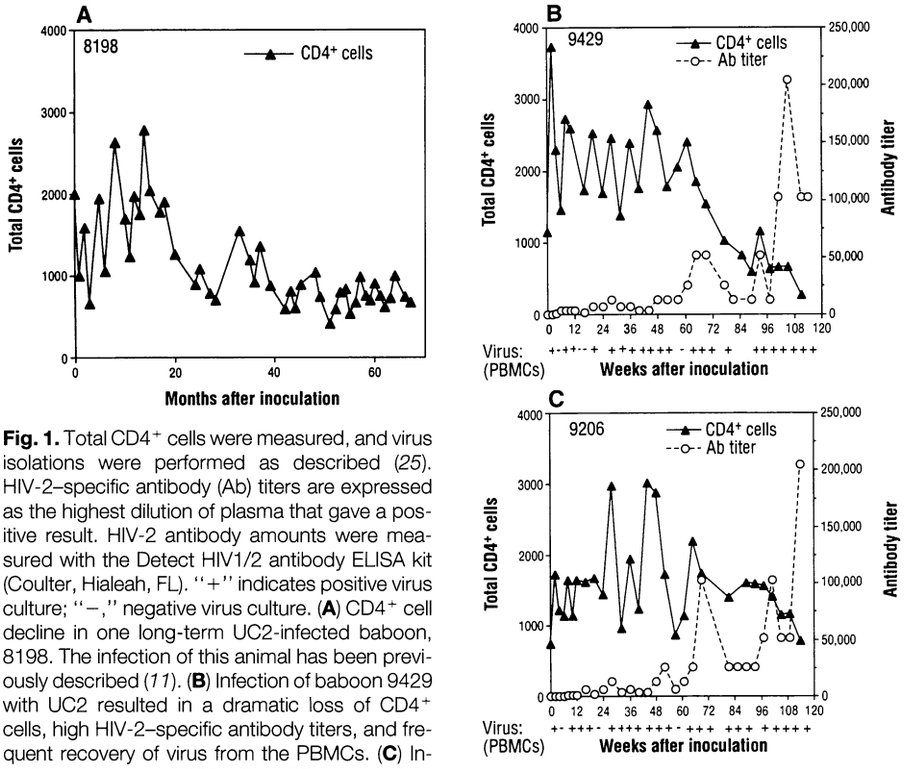

Fig. 1. Total CD4$^+$ cells were measured, and virus isolations were performed as described (*25*). HIV-2–specific antibody (Ab) titers are expressed as the highest dilution of plasma that gave a positive result. HIV-2 antibody amounts were measured with the Detect HIV1/2 antibody ELISA kit (Coulter, Hialeah, FL). "+" indicates positive virus culture; "−," negative virus culture. (**A**) CD4$^+$ cell decline in one long-term UC2-infected baboon, 8198. The infection of this animal has been previously described (*11*). (**B**) Infection of baboon 9429 with UC2 resulted in a dramatic loss of CD4$^+$ cells, high HIV-2–specific antibody titers, and frequent recovery of virus from the PBMCs. (**C**) Infection of baboon 9206 with UC2 resulted in a decline in CD4$^+$ cells, high antibody titers, and frequent recovery of virus from the PBMCs.

Histopathologic examination of the lymph nodes of animal 9429 revealed evidence of follicular lysis and paracortical cell expansion (Fig. 2A). Immunohistochemical staining with B cell–specific antibody to CD20 demonstrated lymphoid depletion in the germinal centers of the lymph nodes from this animal. Follicular depletion is characteristic of the later stages of HIV- and SIV-induced disease in humans and macaques, respectively (*14*). Loss of the function of the follicular dendritic cell network could lead to increased viremia in the blood and rapid progression to disease in HIV-infected individuals (*16*). This pathogenic process could explain the relatively high levels of infectious virus found in the PBMCs of HIV-2–infected baboon 9429 just before and at the time of necropsy (Table 2).

The percentages of CD4$^+$ cells in the lymph nodes of baboon 9429 were dramatically reduced as compared to those of the other infected animals and the uninfected control (Table 2). This reduction was observed at 3 weeks before and at the time of necropsy. In macaques infected with SIV, a decline in lymph node CD4$^+$ cells is not generally observed until the final stages of disease when circulating CD4$^+$/CD8$^+$ cell ratios have fallen to 0.5 or below. This observation is believed to be indicative of the immunological deterioration of the lymph node that eventually leads to in-

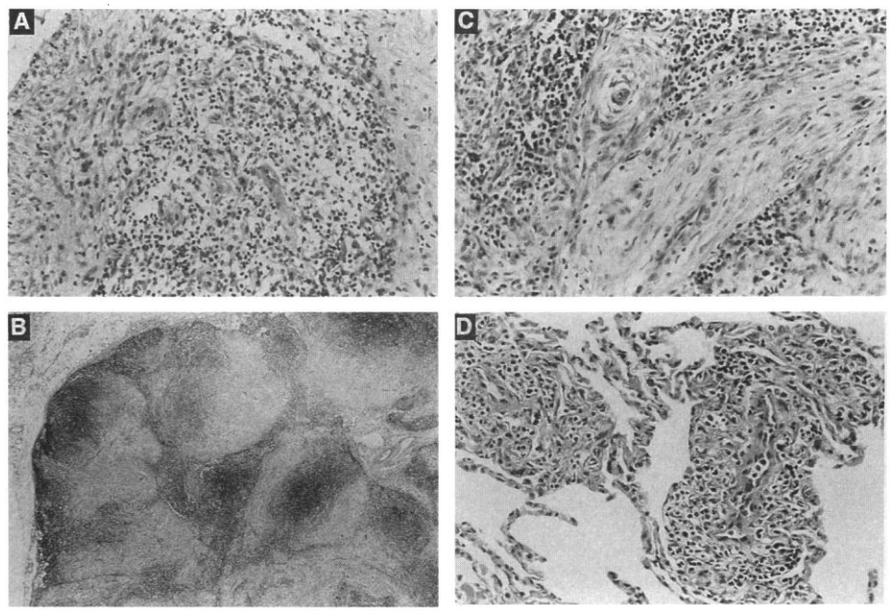

Fig. 2. Histological examination of tissues recovered from HIV-2–infected baboon 9429 at necropsy (magnification ×40). (**A**) Follicular lysis in the lymph node of baboon 9429 recovered at necropsy (hematoxylin and eosin stain). The germinal center shows lymphoid depletion and disruption of the follicular dendritic network, both characteristic of HIV infection. (**B**) Lymph node at lower magnification showing extensive fibrosis. A prominent proliferation of mesenchymal cells was observed in the lymph nodes (and other tissues). This fibromatous tumor did not stain for factor VIII (endothelial cell marker), S100 (neuroectoderm), or keratin (epithelial cell marker). The tumor did stain positive for the myofibroblast marker, smooth muscle actin (SMA; reagents supplied by Dako, Sunnyvale, CA) (*26*). That smooth muscle cells are the origin for Kaposi's sarcoma–derived cells has been proposed (*27*). Immunohistochemical staining with HIV-2$_{ST}$ gp130 antibody and HIV-1 p24 antibodies (Abbott Laboratories, Chicago, IL) did not reveal any virus in the fibromatous tumor. (**C**) Vasocentric fibroblastic tumor in lymph node. The distribution of the proliferation is primarily vasocentric and appears to follow the sinusoidal architecture of the lymph node with frank tumor nodules in paracortical regions of the nodes. This finding supports the origin of the tumor from myofibroblast cells of the vessel wall. (**D**) Lymphocytic interstitial pneumonitis (LIP) as shown in lung tissue. In a diffuse infiltration of alveolar septa with T cells (positive to CD3 antibodies), occasional B cells and plasma cells were observed. Small parabronchial germinal centers consisting of B cells were identified with CD20 antibodies. These histologic findings can be seen in LIP in children (*19*).

creased susceptibility to infections and progression to simian AIDS (SAIDS) (*17*). A similar course of events appears to have occurred in baboon 9429.

It is noteworthy that extensive fibrosis was observed in the skin, lymph nodes, thyroid, and pancreas of baboon 9429 (Fig. 2, B and C). This condition appears to be an abnormal hyperplasia characterized by vasocentric proliferation of fibroblast-like cells in the tissues. This type of tumor has not been reported previously in baboons. A similar fibrosis (retroperitoneal fibromatosis) has been described in macaques with SAIDS associated with infection with the simian retrovirus SRV-2 (*18*). The condition in the macaques has been considered analogous to Kaposi's sarcoma in HIV-infected humans. Serologic evaluation of baboon 9429 showed no evidence of infection with STLV or SRV-2 (Virus Reference Laboratory, San Antonio, TX). Moreover, PBMC cultures from all animals before HIV-2 inoculation showed no evidence of preexisting retroviral infections as measured by reverse transcriptase activity in culture supernatants.

Histopathologic examination of lung tissue from animal 9429 showed evidence of lymphocytic interstitial pneumonitis (Fig. 2D). This disease is characterized by $CD8^+$ lymphocyte infiltration of the lung and is common in HIV-infected children (*19*). This disease alone could have been fatal to this animal if it had not been killed.

Finally, lymph node cells (LNCs) and PBMCs taken from baboon 9429 at 3 weeks before and at the time of necropsy had appreciable virus loads relative to the other infected animals (Table 2). Virus was isolated from the cells of all lymphoid tissues examined, including mesenteric, axillary, mediastinal, and cervical lymph nodes, spleen, bone marrow, and PBMCs. Just before the animal was killed, 1 in 1000 PBMCs and 1 in 1000 LNCs from it were found to harbor infectious virus. This amount represents about 1 in 160 infected $CD4^+$ cells in these tissues at this time. These values are comparable to those observed during the later stages of HIV disease in humans (*16*, *20*). Immunohistochemical examination has further shown viral gp130 and p27 in macrophages in the lymph node, colon, and spleen. This widespread HIV-2 infection of tissues in this animal is an additional feature that resembles end-stage HIV- and SIV-induced diseases in their respective hosts (*21*).

Baboon 9206, another animal in the same group of UC2-infected animals, also demonstrated a noticeable decline in its $CD4^+$ cells (and in its $CD4^+/CD8^+$ cell ratio) after 69 weeks (Fig. 1C). As observed in the case of animal 9429, this decline appeared to correspond to a sharp rise in HIV-2–specific antibody titers in this animal. Moreover, when examined at 2 years and 8 months after inoculation, baboon 9206 was cachectic and had alopecia and multiple fibrous skin lesions similar to those observed in animal 9429 (Table 1). Furthermore, a lymph node biopsy specimen taken from baboon 9206 at this time revealed evidence of follicular lysis. This animal appears to be following a pathogenic course similar to that observed for 9429.

In further studies evaluating the baboon as an experimental model of HIV infection, three additional baboons (8513, 8570, and 8594) were inoculated intravenously with 10,000 $TCID_{50}$ of HIV-2_{UC14} (Table 1). Virus was recovered from all three animals up to 8 weeks after the inoculation. Moreover, in two of these animals (8513 and 8570), infectious virus was isolated from the cell-free plasma during acute infection, indicating extensive replication of UC14 in the baboon. Virus was recovered from the PBMCs of each animal at week 2, and intermittently thereafter from baboons 8570 and 8594. In addition, a high titer of infectious virus was measured in the LNCs of animal 8570 at week 58 (Table 2). All animals seroconverted in 2 to 4 weeks. The successful infection of these baboons with a second genetically distinct strain of HIV-2 (*22*) lends support to the potential usefulness of the baboon model for vaccine studies that require heterologous virus challenge.

Studies now in progress involve serial passage of viruses from both UC2- and UC14-infected baboons into additional animals to select for viral variants that induce a more rapid pathogenic course. Blood was transfused from animals 9429 (UC2-infected) and 8570 (UC14-infected) into each of two previously uninfected baboons. Both animals seroconverted, and virus has been recovered consistently from their PBMCs from 2 weeks to the present time (32 weeks). Furthermore, one of these animals (UC2-infected) showed plasma viremia and lymphoid hyperplasia in the lymph node at week 8. The lymph node of the other animal (UC14-infected) also showed lymphoid hyperplasia and yielded virus by culture at this time.

Here, we showed that baboons have been successfully infected with two different strains of HIV-2. These infections have been characterized by frequent virus isolations from the PBMCs and lymph nodes, lymphadenopathy, plasma viremia, and high HIV-2–specific antibody titers. Our observations indicate viral persistence in most of these animals. In three cases, a decline in total $CD4^+$ cells was observed at about 18 months after inoculation. In one

Table 2. Detection of HIV-2 in lymphoid tissues and PBMCs from infected baboons. LNCs were recovered from the inguinal (ing.), cervical (cerv.), mediastinal (med.), axillary (ax.), and mesenteric (mes.) lymph nodes at the indicated times after inoculation. We performed infectious center assays by cocultivating these LNCs or baboon PBMCs at varying cell densities (10^2 to 10^6 cells) with 10^6 PHA-stimulated human PBMCs in a 24-well plate. Infectious center titers represent the lowest cell density of baboon cells that yielded a positive virus culture. "+" indicates a positive virus culture when 3×10^6 cells were cocultured with human PBMCs; "−" indicates no virus recovery from a similar culture. Culture supernatants were monitored for virus at 3- to 7-day intervals with either the HIV-1 p24 ELISA (Coulter, Hialeah, FL) or the RT assay (*24*). The percentage of $CD4^+$ cells was determined as described (*25*).

Animal	Virus	Week	Tissue	Infectious center titer	$CD4^+$ cells (%)
			Tissue specimens		
9429	UC2	111	LNC-ing.	10^3	16.4
			PBMC	10^3	16.0
9206	UC2	119	LNC-ing.	+	53.0
			PBMC	10^5	29.4
9168	UC2	119	LNC-ing.	−	42.0
			PBMC	−	27.4
8387	UC2	119	LNC-ing.	−	58.0
			PBMC	−	25.7
8570	UC14	58	LNC-ing.	10^3	55.0
			PBMC	10^6	32.8
7796	Control	111	LNC-ing.	−	60.9
			PBMC	−	51.2
			Necropsy specimens		
9429	UC2	114	Spleen	+	1.97
			Thymus	+	46.08
			LNC-cerv.	10^5	15.36
			LNC-med.	10^4	14.95
			LNC-ing.	10^4	12.03
			LNC-ax.	10^5	15.6
			LNC-mes.	+	12.02
			PBMC	10^3	10.94

baboon with a high virus load in its PBMCs, widespread infection of lymphoid tissues, and a dramatic loss of $CD4^+$ lymphocytes, clinical signs and symptoms including extensive fibromatosis were observed. Moreover, a second HIV-2–infected animal appears to be following a similar clinical course. These features closely resemble those in human and simian AIDS. Although other investigators have shown that baboons are susceptible to infection with HIV-2 strains (*23*), our results show viral persistence and pathogenesis in this animal. HIV-2 infection of baboons thus offers a promising, reproducible, and affordable animal model for studies of HIV persistence and pathogenesis. This model is particularly important when protection against infection, as well as disease development, must be assessed.

REFERENCES AND NOTES

1. H. J. Alter *et al.*, *Science* **226**, 549 (1984); P. N. Fultz *et al.*, *J. Virol.* **58**, 116 (1986); W. J. W. Morrow *et al.*, *AIDS Res. Hum. Retrovir.* **5**, 233 (1989).
2. M. B. Agy *et al.*, *Science* **257**, 103 (1992).
3. Current prices for chimpanzees are $30,000 to $65,000 per animal; rhesus monkeys and pig-tailed macaques are $3,000 to $4,000 each, and the latter are in limited supply. In contrast, baboons presently cost $1100 to $1800 and are in plentiful supply. Moreover, they are easily imported into the United States.
4. L. R. Frumkin *et al.*, *Virology* **195**, 422 (1993).
5. E. Cortes *et al.*, *N. Engl. J. Med.* **320**, 953 (1989); T. R. O'Brien, J. R. George, S. D. Holmberg, *J. Am. Med. Assoc.* **267**, 2775 (1992); P. G. Babu, N. K. Saraswathi, F. Devapriya, T. J. John, *Indian J. Med. Res.* **97**, 49 (1993); M. Grez *et al.*, *J. Virol.* **68**, 2161 (1994).
6. V. M. Hirsch, R. A. Olmsted, M. Murphey-Corb, R. H. Purcell, P. R. Johnson, *Nature* **339**, 389 (1989); M. Peeters, P. Piot, G. van der Groen, *AIDS* **5**, S29 (1991).
7. R. C. Desrosiers, *Annu. Rev. Immunol.* **8**, 557 (1990); M. B. Gardner and P. A. Luciw, *Fed. Am. Soc. Exp. Biol. Proc.* **3**, 2593 (1989).
8. J. Li, C. I. Lord, W. Haseltine, N. L. Letvin, J. Sodroski, *J. Acquired Immune Defic. Syndr.* **5**, 639 (1992); R. Shibata and A. Adachi, *AIDS Res. Hum. Retrovir.* **8**, 403 (1992).
9. P. Putkonen *et al.*, *J. Acquired Immune Defic. Syndr.* **2**, 366 (1989); C. Stahl-Hennig *et al.*, *AIDS* **4**, 611 (1990); J. Livartowski *et al.*, *Cancer Detect. Prev.* **16**, 341 (1992).
10. J. McClure *et al.*, abstract, Tenth Annual Symposium on Nonhuman Primate Models for AIDS, San Juan, Puerto Rico, 1992.
11. B. A. Castro, M. Nepomuceno, N. W. Lerche, J. W. Eichberg, J. A. Levy, *Virology* **184**, 219 (1991).
12. The UC2 strain was originally recovered from a dually infected individual after its passage in the CEM T lymphoblastoid cell line [L. Evans, *Lancet* **ii**, 1389 (1988)]. The UC3 strain more closely resembles a primary isolate in that it has been passaged only in human PBMCs. UC3 is described elsewhere (*11*).
13. UC12 and UC14 are primary HIV-2 isolates recovered from patients from the Gambia (S. W. Barnett, H. Whittle, J. A. Levy, unpublished results).
14. P. Racz *et al.*, *Prog. Allergy* **37**, 81 (1986); L. V. Chalifoux *et al.*, *Am. J. Pathol.* **128**, 104 (1987); D. J. Ringler *et al.*, *ibid.* **134**, 373 (1989); M. S. Wyand *et al.*, *ibid.*, p. 385.
15. D. Blackbourn, S. W. Barnett, J. A. Levy, unpublished observations.
16. G. Pantaleo *et al.*, *Nature* **362**, 355 (1993); J. Embretson *et al.*, *ibid.*, p. 359.
17. Y. J. Rosenberg *et al.*, *AIDS Res. Human Retrovir.* **9**, 639 (1993).
18. K. Stromberg *et al.*, *Science* **224**, 289 (1984); P. A. Marx *et al.*, *J. Virol.* **56**, 571 (1985).
19. A. S. Teirstein and M. J. Rosen, *Clin. Chest Med.* **9**, 467 (1988); S. A. Schroeder *et al.*, *Chest* **101**, 1065 (1992).
20. S. M. Schnittman *et al.*, *Science* **245**, 305 (1989); K. Hsia and S. A. Spector, *J. Infect. Dis.* **164**, 470 (1991).
21. V. M. Hirsch, P. M. Zack, A. P. Vogel, P. R. Johnson, *J. Infect. Dis.* **163**, 976 (1991); Y. K. Donaldson *et al.*, *Lancet* **343**, 382 (1994).
22. DNA sequence analysis of UC2 and UC14 in the C2-V3 region of their Env coding regions revealed only 82% amino acid identity.
23. N. L. Letvin *et al.*, *J. Infect. Dis.* **156**, 406 (1987); I. Nicol *et al.*, *Intervirology* **30**, 258 (1989).
24. A. D. Hoffman, B. Banapour, J. A. Levy, *Virology* **147**, 326 (1985).
25. Baboons were inoculated intravenously with 5000 $TCID_{50}$ of UC2 or 10,000 $TCID_{50}$ of UC14 on the given dates. HIV-2 strains were prepared and titrated in human PBMCs obtained from human seronegative donors [S. Barnett, *J. Virol.* **67**, 1006 (1993)]. The PBMCs from all animals were prescreened for in vitro susceptibility to virus infection (*11*). All inoculations and animal manipulations were performed according to NIH guidelines at the Southwest Foundation for Biomedical Research (San Antonio, TX). Every 2 weeks for 12 weeks, then at 4-week intervals, animals were sedated with ketamine hydrochloride (10 mg per kilogram of body weight) and examined for hepatomegaly or splenomegaly, lymphadenopathy, fever, weight loss, and cutaneous signs. At these times, venipuncture was performed and blood specimens collected. Virus isolations were performed by cocultivation of the PBMCs of infected animals with phytohemagglutinin (PHA)-stimulated PBMCs from seronegative human donors as previously described (*11*). Culture supernatants were monitored for virus at 3- to 4-day intervals with either the HIV-1 p24 enzyme-linked immunosorbent assay (ELISA) (Coulter, Hialeah, FL) or the reverse transcriptase (RT) assay (*24*). In some cases, $CD4^+$ baboon PBMCs were purified with CD4 antibody immunomagnetic beads (Dynal, Lake Success, NY) before cocultivation with human PBMCs [C. Mackewicz, *J. Clin. Invest.* **87**, 1462 (1991)]. Fresh plasma specimens were assayed for infectious virus within 3 hours after collection by inoculation onto human PBMCs [L. Pan, *J. Clin. Microbiol.* **31**, 283 (1993)]. T cell subsets were measured by flow cytometry with the leu3a (CD4) and leu2a (CD8) monoclonal antibodies (Becton Dickinson, San Jose, CA).
26. B. G. Herndier *et al.*, *AIDS* **8**, 575 (1994).
27. A. Albini, C. D. Mitchell, E. W. Thompson, *J. Cell. Biochem.* **36**, 369 (1988).

28. The authors thank Y.-D. Sun, S. Lunceford, S. Rouse, D. Johnson, and N. Abbey for their excellent technical assistance. We also thank D. Kilhorn for administrative assistance and C. Beglinger for her help in preparing the manuscript. The HIV-2_{ST} gp130 antibody was provided by SmithKline Beecham, King of Prussia, PA. Supported by NIH grant U01-AI26471 and the UCSF AIDS Clinical Research Center, funded by the California State University AIDS Research Program. S.W.B. was a Scholar of the American Foundation for AIDS Research.

8 June 1994; accepted 30 August 1994

Design of a G·C–Specific DNA Minor Groove–Binding Peptide

Bernhard H. Geierstanger, Milan Mrksich, Peter B. Dervan,* David E. Wemmer*

A four-ring tripeptide containing alternating imidazole and pyrrole carboxamides specifically binds six–base pair 5′-(A,T)GCGC(A,T)-3′ sites in the minor groove of DNA. The designed peptide has a specificity completely reversed from that of the tripyrrole distamycin, which binds A,T sequences. Structural studies with nuclear magnetic resonance revealed that two peptides bound side-by-side and in an antiparallel orientation in the minor groove. Each of the four imidazoles in the 2:1 ligand-DNA complex recognized a specific guanine amino group in the GCGC core through a hydrogen bond. Targeting a designated four–base pair G·C tract by this synthetic ligand supports the generality of the 2:1 peptide-DNA motif for sequence-specific minor groove recognition of DNA.

During the past decade, efforts to alter the sequence specificity of naturally occurring small molecules that bind to the minor groove of DNA have met with limited success (*1*, *2*). The natural products netropsin and distamycin are *N*-methylpyrrole–containing di- and tripeptides that bind in the minor groove at sites of at least four successive A·T base pairs (*1*, *3*–*6*). Inspired by the x-ray structure of the 1:1 complex of netropsin with A,T-rich DNA (*4*), efforts were initiated to synthesize ligands capable of recognizing G,C-containing sequences through specific hydrogen bonding to the guanine amino group in the minor groove (*7*, *8*). Initial attempts based on the 1:1 complex led to molecules with increased tolerance for G·C base pairs in the binding site, but not to high specificity (*7*). The limitations of this approach became apparent when it was realized that two distamycin molecules could be combined side-by-side in the minor groove of DNA (*9*–*11*). The 2:1 binding mode had been observed for peptide analogs containing a single imidazole or pyridine ring, which bind sequences containing both A·T and G·C base pairs, emphasizing the importance of the sequence-dependent

B. H. Geierstanger and D. E. Wemmer, Graduate Group in Biophysics and Department of Chemistry, University of California, Berkeley, CA 94720, USA.
M. Mrksich and P. B. Dervan, Arnold and Mabel Beckman Laboratories of Chemical Synthesis, California Institute of Technology, Pasadena, CA 91125, USA.

*To whom correspondence should be addressed.